Paper-based plasma sanitizers

Jingjin Xie[a], Qiang Chen[b], Poornima Suresh[a], Subrata Roy[c], James F. White[b], and Aaron D. Mazzeo[a,1]

[a]Department of Mechanical and Aerospace Engineering, Rutgers University, Piscataway, NJ 08854; [b]Department of Plant Biology, Rutgers University, New Brunswick, NJ 08901; and [c]Department of Mechanical and Aerospace Engineering, University of Florida, Gainesville, FL 32611

Edited by John A. Rogers, University of Illinois, Urbana, IL, and approved March 28, 2017 (received for review December 23, 2016)

This work describes disposable plasma generators made from metallized paper. The fabricated plasma generators with layered and patterned sheets of paper provide a simple and flexible format for dielectric barrier discharge to create atmospheric plasma without an applied vacuum. The porosity of paper allows gas to permeate its bulk volume and fuel plasma, while plasma-induced forced convection cools the substrate. When electrically driven with oscillating peak-to-peak potentials of ±1 to ±10 kV, the paper-based devices produced both volume and surface plasmas capable of killing microbes. The plasma sanitizers deactivated greater than 99% of *Saccharomyces cerevisiae* and greater than 99.9% of *Escherichia coli* cells with 30 s of noncontact treatment. Characterization of plasma generated from the sanitizers revealed a detectable level of UV-C (1.9 nW·cm^{-2}·nm^{-1}), modest surface temperature (60 °C with 60 s of activation), and a high level of ozone (13 ppm with 60 s of activation). These results deliver insights into the mechanisms and suitability of paper-based substrates for active antimicrobial sanitization with scalable, flexible sheets. In addition, this work shows how paper-based generators are conformable to curved surfaces, appropriate for kirigami-like "stretchy" structures, compatible with user interfaces, and suitable for sanitization of microbes aerosolized onto a surface. In general, these disposable plasma generators represent progress toward biodegradable devices based on flexible renewable materials, which may impact the future design of protective garments, skin-like sensors for robots or prosthetics, and user interfaces in contaminated environments.

paper-based electronics | plasma | touch sensors | kirigami | sanitization

State-of-the-art, plasma generators are capable of manipulating surface chemistries in manufacturing processes (1, 2), sterilizing medical devices (3, 4), providing thrust for space vehicles (5, 6), manipulating lift-to-drag ratios on airfoils (7, 8), manipulating heat transfer (9), healing wounds (10), and killing microbes in atmospheric environments (11, 12). These plasma-based generators typically use rigid components, which cannot bend or conform to irregularly shaped objects. The lack of flexibility limits their potential use as protective skins for prosthetics, wearable garments, robotics, or hard-to-access areas where microbes might collect. In addition, chamber-free ionizers with atmospheric plasma typically have small active areas (~50 cm^2) not designed for scalable antimicrobial protection over large surfaces. Scalable and flexible atmospheric plasma generators might be suitable in varied urban and rural environments to reduce healthcare-associated infections.

Previous studies have suggested that plasma generators have the potential to be fast, efficient, and safe devices for healing wounds (10, 13), modifying structural surfaces (14), and assisting in tissue engineering (15). In general, plasma-based sanitization/disinfection/sterilization takes advantage of three synergistic mechanisms: (*i*) interacting free radicals, (*ii*) radiative effects from UV light, and (*iii*) volatilization of microorganisms (16). Sanitization reduces the number of disease-causing microbes, disinfection provides further reduction, and sterilization is the most stringent form of decontamination with demonstrated deactivation of spores. Plasma-based treatments have the potential to provide comparable sterilization to conventional methods that use heat (17), chemicals (17), or radiation (18–21). Plasma treatments have deactivated a range of microbes, such as *Geobacillus stearothermophilus* (22), *Staphylococcus aureus* (MRSA) (23), and adenoviruses (24) on varied substrates [e.g., food (25)].

Cellulose-based paper has tunable porosity to allow gases to permeate its bulk volume, and it is capable of handling temperatures up to 250 °C (26). These properties make paper a fitting material for atmospheric plasma generators, as its permeability allows the flow of gas through the substrate to provide fuel for the plasma and to cool the paper with plasma-induced forced convection. Stemming from advances in paper-based microfluidics (27–29), paper-based electronics and photonics (papertronics) are demonstrating advances in energy, sensing, actuation, communication, and biodiagnostic applications (30–34). There is a gradual transition from conventional, nonresponsive paper products (e.g., printing, food packaging, labels, and decorations) to active, communicative, and "smart" devices (35–38).

In this work, we report the design, fabrication, and experimental characterization of a simple and disposable plasma generator that is mechanically flexible and capable of antimicrobial sanitization. Beyond characterizing the effectiveness of the sanitizers, this work also demonstrates garment-like protection, multifunctional capacitive touchpads, and a kirigami-based "stretchy" device. Potential applications of kirigami-based, stretchable plasma generators might include comfortable protective garments. Ultimately, the engineering and science demonstrated in this work is a step toward large-scale, skin-like sensors that provide active antimicrobial protection.

Experimental Design

Fabrication of Plasma-Generating Devices. For each paper-based plasma generator, we prepared two 150-μm sheets of metallized

Significance

Conventional plasma-based treatments deactivate microbes in confined, nonatmospheric chambers. During the last few decades, new concepts have led to portable, chamberless generators with rigid configurations of electrodes. This work explores unique designs and methods of antimicrobial sanitization with flexible plasma generators consisting of laminated assemblies of patterned, metallized paper. Under oscillating potentials (±1 to ±10 kV from 100 Hz to 8 kHz), the paper-based devices produced plasma that deactivated 99% of *Saccharomyces cerevisiae* and *Escherichia coli* cells with 30 s of treatment. Future uses of this type of plasma generator might include the sanitization of protective garments, origami- or kirigami-like devices, and human–machine user interfaces in healthcare and/or contaminated environments.

Author contributions: J.X., Q.C., S.R., J.F.W., and A.D.M. designed research; J.X., Q.C., P.S., J.F.W., and A.D.M. performed research; J.X., Q.C., S.R., J.F.W., and A.D.M. analyzed data; and J.X., Q.C., S.R., J.F.W., and A.D.M. wrote the paper.

Conflict of interest statement: US Provisional Patent was filed (62/291,082) for "Low-Cost, Flexible, Paper-Based Plasma Sterilizer" on February 4, 2016. US Patent Application was filed (15/425,474) for "Flexible Plasma Applicators Based on Fibrous Layers" on February 6, 2017.

This article is a PNAS Direct Submission.

[1]To whom correspondence should be addressed. Email: aaron.mazzeo@rutgers.edu.

This article contains supporting information online at www.pnas.org/lookup/suppl/doi:10.1073/pnas.1621203114/-/DCSupplemental.

paper (A-550; AR Metallizing) patterned with a laser engraver (VLS 2.3; Universal Laser Systems). Fig. 1 depicts the laminated structure of the devices and the metallized paper. In this study, we engraved repeated hexagons (honeycombs) on the devices. Such a pattern uses a minimal amount of total perimeter to cover a surface (39) and permits generation of atmospheric plasma along the edges of the hexagonal grid. By tuning the size/spacing of the honeycombs, it is possible to ensure the plasma has coverage over the entirety of a patterned surface.

As illustrated in Fig. 1*A*, we bonded the nonconductive sides of two sheets of laser-engraved metallized paper with a 30-μm-thick adhesive layer (Ad-Tech 5645; Adhesive Technology). To connect the patterned conductive regions to an external power supply, we bonded wires to the metallized paper with water- and silver-based inks (Conductive Compounds Company) in similar fashion to that described in ref. 35.

Generation of Plasma. The paper-based plasma generators in this work rely on the working principle of dielectric barrier discharge (DBD). The first demonstration of DBD-based plasma was in 1857 by Siemens (14), but the first report of DBD for deactivation of microbes was not until the mid-1990s (40). The plasma originates from the discharge between two electrodes separated by a dielectric medium, which, in our work, is a porous matrix of cellulose fibers. To produce plasma, we first produced sinusoidal signals with frequencies ranging from 1 to 8 kHz and peak-to-peak voltages $V_{p\text{-}p}$ ranging from ±1 to ±5 V using a function generator (4011A; BK Precision). Then, we amplified this signal using a high-voltage amplifier (model 10/10; TREK) with a gain of 1,000 to output a high oscillating potential $V_{p\text{-}p}$ ranging from ±1 to ±5 kV. The generation of plasma was also frequency dependent, which suggests the existence of an optimal frequency at a given electric potential to generate uniform coverage of plasma (Movie S1). The power consumptions for typical paper-based plasma generators demonstrated in this work were less than 20 W (~18 W for RMS 2.2 kV at ~8 mA) going into the device.

DBD can produce two types of plasma (i.e., volume plasma and surface plasma) depending on the configuration of the device. Although both configurations consist of one or more dielectric insulators sandwiched by two electrodes, volume plasma usually has a gap of air between the two electrodes, whereas surface plasma does not. The plasma presented in this work was a combination of both volume plasma and surface plasma because of the porosity of the metallized paper. Fig. 1*A* illustrates the typical geometry and locations of the volume and surface plasmas.

The paper-based plasma generators produced glowing plasma and perceptible ozone. Fig. 1*C* shows a flexible, functioning plasma generator in the form of a logotype with an internally etched, honeycomb pattern. This sample was under the excitation of a peak-to-peak voltage of ±3 kV at 1.7 kHz. Fig. 1*D* shows another functioning rectangular plasma generator conforming to a cylindrical substrate (diameter of ~100 mm) while generating glowing plasma activated with a peak-to-peak voltage $V_{p\text{-}p}$ of ±2 kV at 1 kHz. Characterization of the plasma (*Supporting Information*) also showed a detectable level of UV-C (1.9 $nW{\cdot}cm^{-2}{\cdot}nm^{-1}$; Fig. S1), modest surface temperature (60 °C with 60 s of activation; Fig. S2*B*), and a high level of ozone (13 ppm with 60 s of activation; Figs. S2*A* and S3 and Table S1).

Noncontact Experiments. To characterize the efficacy of paper-based plasma sanitizers, we performed experimental studies with two setups (i.e., a noncontact experiment and a direct-contact experiment for both *Saccharomyces cerevisiae* and *Escherichia coli*). In noncontact experiments, we prepared circular plasma sanitizers with metallized paper and measured the ozone levels (*Supporting Information*). Each sanitizer had a diameter of 90 mm,

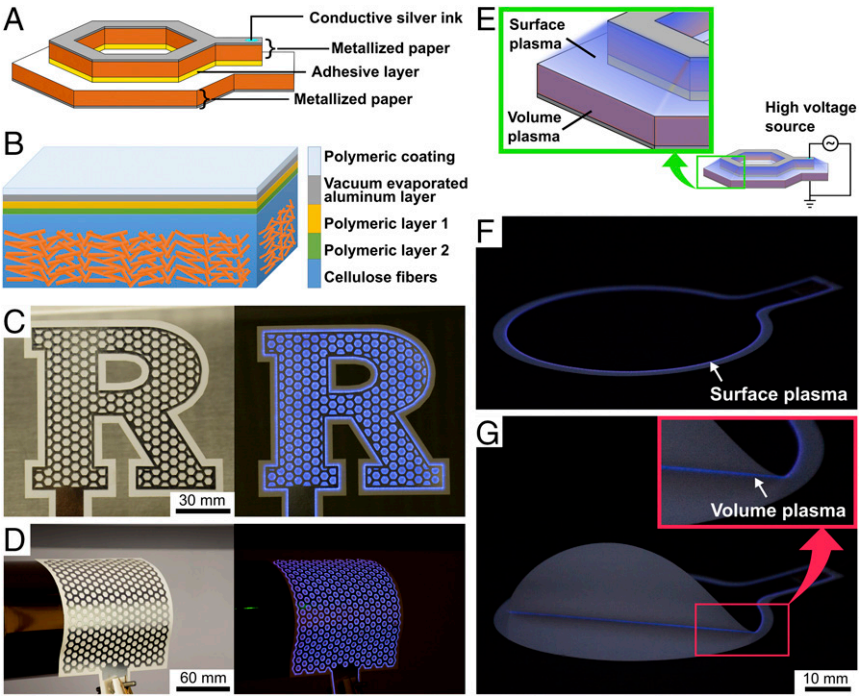

Fig. 1. Atmospheric plasma generators made from metallized paper. (*A*) A hexagonal unit of a paper-based plasma generator. (*B*) The laminated structure of metallized paper used in this work. (*C*) A paper-based plasma generator with and without applied potential. (*D*) A flexible plasma generator made from etched metallized paper in straight and bent states. (*E*) Volume plasma goes through the porous matrix of cellulose-based fibers, while surface plasma is above/below the metallized substrate. (*F*) A flat, circular plasma generator without patterned honeycombs shows surface plasma. (*G*) A circular plasma generator with the same design as *F* has one-half of the top layer curling upward to demonstrate the production of both volume and surface plasmas. The plasma glowed with the application of a $V_{p\text{-}p}$ of ±3 kV at 1.7 kHz for *C*, a $V_{p\text{-}p}$ of ±2 kV at 1 kHz for *D*, and a $V_{p\text{-}p}$ of ±2.5 kV at 2 kHz for *F* and *G*.

matching the inner diameter of the lid of a Petri dish. By attaching the sanitizer to the inner surface of the lid, we avoided touching the sanitizer during experiments, which would have led to unintentional contamination. When closed, the surface of the paper-based sanitizer was 10 mm away from the surface of the yeast extract–peptone–dextrose (YEPD) and Luria–Bertani (LB) solid media, on which the *S. cerevisiae* or *E. coli* suspension was inoculated aseptically in the Petri dish. Fig. 2 *A* and *B* illustrates the setup of the noncontact experiments.

We inoculated 100 μL of *S. cerevisiae* and *E. coli* cell suspensions on YEPD and LB solid media, respectively, and then covered the Petri dish with the plasma generator attached to the lid. The lead of the circular sanitizer ran through the gap between the lid and the Petri dish to an AC input with a frequency of 2 kHz and a peak–peak voltage of ±3.15 kV. There were six groups of experiments with varied times of exposure, each consisting of five repetitive samples for both *S. cerevisiae* and *E. coli.*

Direct-Contact Experiments. Our noncontact experiments demonstrated the ability to deactivate bacteria on agar a set distance away from the sanitizers. Nonetheless, it is desirable to deactivate microbes that have landed on a substrate itself. Keypads, shared user interfaces, clothing, and garments exemplify direct-contact applications involving surface contamination with microbes.

A human sneeze is one method of spreading infectious microbes. To simulate a sneeze—an abrupt expulsion of secretions, saliva, and microorganisms from the respiratory tract—and evaluate the efficacy of paper-based plasma generators in decontaminating themselves, we developed an experimental setup (Fig. 3*A*) with a pneumatic dispensing system (Performus II; Nordson EFD). Using a gauge pressure of 11 psi and a dispensing time of 50 μs, an intranasal drug delivery device (MAD Nasal; LMA) aerosolized a liquid suspension of *S. cerevisiae* or *E.coli* onto our paper-based plasma generators. The fine mist of generated droplets had diameters ranging from ∼30 to 100 μm. Having a diameter less than 100 μm, these droplets are similar in size to 95% of droplets in a sneeze (41).

Results and Discussion

Noncontact Experiments. The plasma generators applied treatments for 0 (control), 5, 10, 20, 30, and 60 s. Immediately after timed treatment, we incubated each sample at 30 °C for 48 h. Fig. 2*D* shows the resulting quantities of colonies of *S. cerevisiae* after incubation. After 10 s of active treatment, the mean number of colonies decreased to 16.14, or an inactivation rate of 91.85%. After 20 and 30 s of treatment, the inactivation rate for yeast became 97.89% and 99.34%, respectively. Fig. 2*E* shows the efficacy of using plasma to kill *E. coli*. With only 10 s of treatment, the resulting inactivation rate was as high as 99.93%. Treatments longer than 10 s resulted in an average of less than one remaining colony, representing efficiencies greater than 99.9%. Fig. 2*C* shows the comparison between the control group and the 10-s group of *E. coli*. These results for both *S. cerevisiae* and *E. coli* indicate efficiencies as high as 99% with plasma treatment for only 30 s.

One of the common measures in microbiology is the decimal reduction time, or *D* value. As shown in Eq. 1, it is the time *t* required to inactivate 90% of the cells of a given microorganism in a medium at a specified temperature:

$$D \text{ value} = \frac{t}{\log N_0 - \log N_t}, \quad [1]$$

where N_0 is the initial population and N_t is the population at the end of the test. Based on the experimental results, the *D* values for both *S. cerevisiae* and *E. coli* were less than 10 s.

Direct-Contact Experiments. After dispensing suspensions of *S. cerevisiae* or *E. coli* directly onto the honeycomb-patterned side of a circular paper-based generator, we activated plasma for 0 (control), 5, 10, 20, 30, and 60 s. Then, we transferred the cells attached to the surface of the plasma generator onto a solid media of YEPD or LB. During transfer, we manually applied pressure to the back of the generator for 10 s, and then discarded the generator after use. The inoculated media stayed in the oven at a temperature of 30 °C for 48 h. We also adopted a blank control (BC) group, which contained the same type of paper-based plasma generator but was not activated. Fig. 3*B* shows quantitative results from sanitizing *S. cerevisiae* in the direct-contact experiments. With 60 s of plasma treatment, there were no observable cells on the YEPD media.

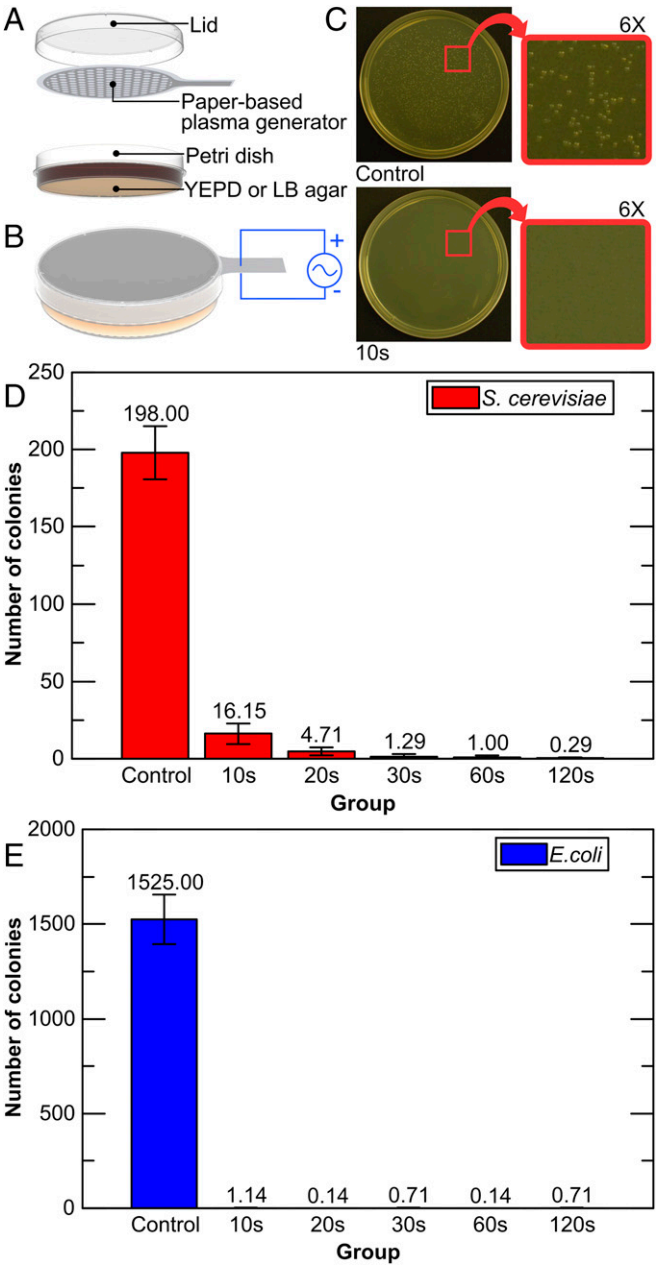

Fig. 2. Experimental setup for verifying the efficiency of noncontact sanitization using the designed paper-based plasma generators. (*A*) Exploded view of the setup: a circular paper-based plasma generator with hexagonal patterns fits the lid of a Petri dish. (*B*) The assembly of the setup when conducting experiments. (*C*) Images of experiments with *E. coli* showing the comparison of a control group and a sample after 10 s of treatment. (*D*) Plotted number of colonies versus sanitization time for *S. cerevisiae* cells. (*E*) Plotted number of colonies versus sanitization time for *E. coli*.

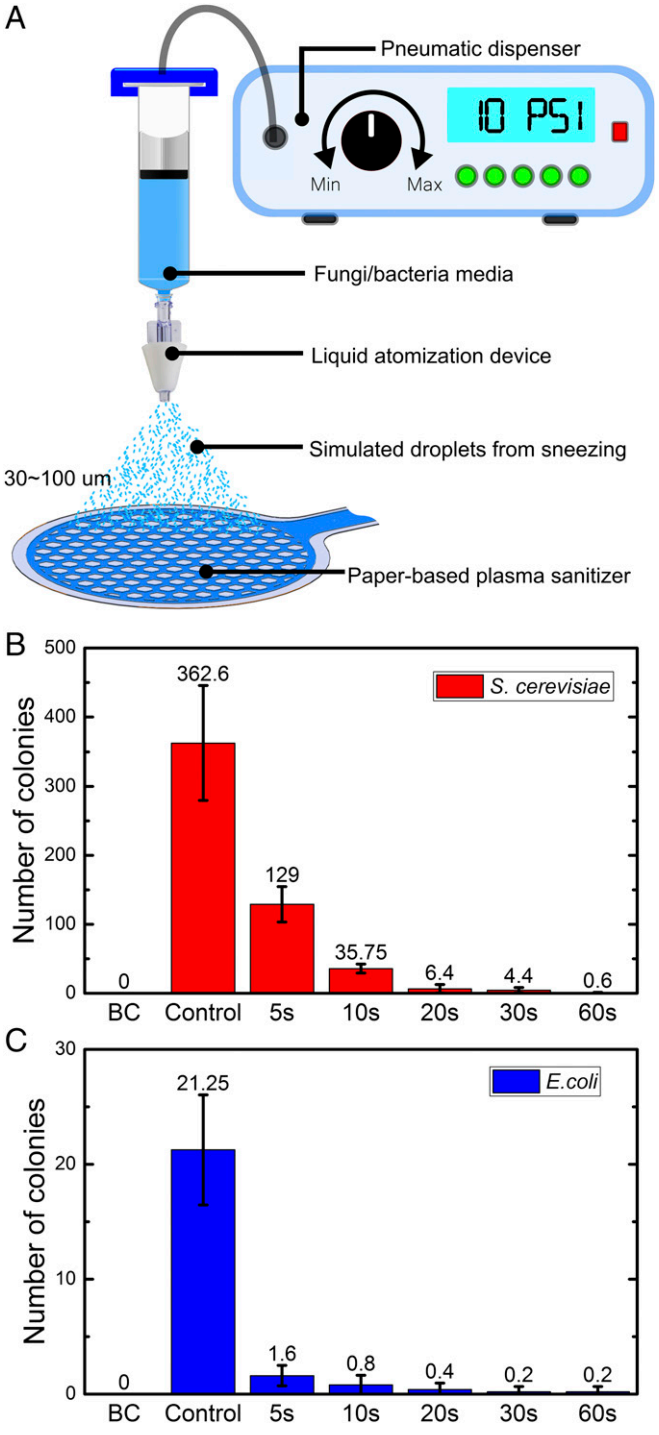

Fig. 3. Experimental results showing the efficiency of paper-based plasma sanitizers exposed to aerosolized liquid suspensions of *S. cerevisiae* and *E. coli*. (*A*) Setup used in direct-contact experiments. (*B*) A histogram showing the number of colonies formed by *S. cerevisiae* after being incubated for 48 h. (*C*) A histogram showing the number of colonies formed by *E. coli* after being incubated for 48 h. BC, blank control.

Fig. 3*C* shows the quantitative results from sanitizing *E. coli* in the direct-contact experiments. With only 10 s of treatment, there were no observable colonies on the LB media.

Contamination and Self-Sanitization of Metallized Paper. Metallized paper, generally used for labeling and printed media, is not an inherently sterile product. Thus, the metallized paper likely possessed contaminants on its surfaces and within its porous structure. When examining the experimental results, we observed nonspecific contaminants/colonies (i.e., microbes not associated with *E. coli* or *S. cerevisiae*). By examining the DNA sequence of the unspecified colonies, we identified them as *Bacillus*, a type of bacteria that can be difficult to irradiate with chemical solvents, such as isopropyl alcohol. In our experiments, there were two control groups: one with inoculation and one without inoculation. In both control groups, we found some of the media had *Bacillus* contamination. However, none of the samples appeared to be contaminated after 30 s of active plasma. Thus, experimental results suggest that, by generating volume plasma, the metallized paper also treated itself and removed *Bacillus* from its fibrous interior. This result is particularly notable because *Bacillus* species are generally difficult to kill due to the production of resistant endospores.

Paper-Based Disposable Garments. After exposure to hazardous microbes, self-sanitizing garments might decontaminate themselves before being transported offsite and reduce the risk of harmful release of contaminated materials during shipping. In addition, low-cost plasma generators may reduce the rate of morbidity and mortality resulting from nosocomial infections (i.e., diseases or infections acquired in a hospital or healthcare facility) (42). After the outbreak of the highly contagious Ebola virus, there was an increased interest in developing viable, cost-effective techniques for disinfection and enhanced personal protection equipment (43–45).

We have experimentally characterized the effectiveness of paper-based plasma generators for active antimicrobial sanitization. To demonstrate the potential use of the devices in garment-like systems, we prepared a rectangular, paper-based band with one-half of the surface area covered with a hexagonal, conductive layer. There was no conductive layer on the other half as we removed it with laser ablation. This design produced plasma on only one-half of the surface area and reserved the other half as a control group with Kapton tape attached to its surface. Fig. 4 *A* and *D* shows the configuration. In the experiments, we first wrapped the paper-based band around a researcher's wrist, and then carefully sprayed an aerosolized suspension of *E. coli* on the surface of the band to ensure approximately equal distribution of the *E. coli*. The concentration of the suspension was $\sim 3 \times 10^8$ cells/mL. Then, we removed the band from the wrist and connected the electrodes. Fig. 4 *B–D* depicts these steps. After activating the atmospheric plasma, we removed the electrodes and transferred the cells to the surface of a preprepared LB medium. Finally, we incubated the medium at 37 °C for 48 h. Fig. 4*E* shows the results. Movie S2 shows the experiment in motion.

Scalability. Within the limits on the size of acquired metallized paper and working area of the laser engraver, we created paper-based, plasma generators with dimensions up to 400 mm × 276 mm, which is ∼20 times larger than the logotype-based, plasma generator shown in Fig. 1*C*. For the device shown in Fig. 5*A*, the frequency of excitation (100 Hz at a voltage $V_{p\text{-}p}$ of ±3kV) to generate plasma was much lower than that used with the smaller devices previously described. As the electrical resistance scales with the size of the device, especially considering the 10-nm-thick layer of aluminum in the metallized paper (35), this observation agrees with previously reported methods of decreasing the frequency of applied voltage to generate plasma through resistive barrier discharge (46).

Self-Sanitizing Capacitive Touchpad. Based on previously developed capacitive touch sensors, we etched traces to fabricate a keypad (35). By integrating atmospheric plasma generators with this keypad, these devices can potentially sanitize themselves after being touched. Fig. 5*B* shows a sequential operation, including touching the button with two fingers to activate corresponding LEDs, and activating the plasma to sanitize the buttons with a

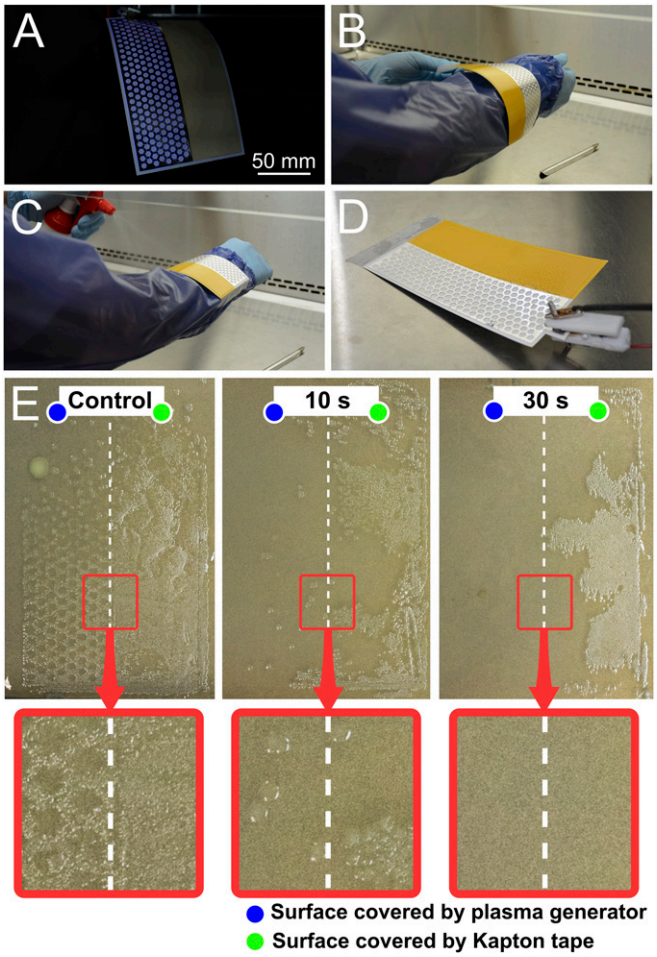

Fig. 4. A paper-based plasma generator as a potential protective garment. (*A*) A rectangular (166 mm × 100 mm) device is in the activated state. The left-hand side has coverage with plasma under the excitation of an AC source with a peak–peak voltage of ±2.3 kV and a frequency of 1.7 kHz. The right-hand side had a layer of Kapton tape, which prevented the generation of plasma as it cut off the supply of air. *B* and *C* show the procedure for spraying the atomized *E. coli* suspension to the paper-based garment. (*D*) An image of the unfolded device attached to the a high-voltage connector. (*E*) The growth of *E. coli* after being transferred to LB agar and incubation for 48 h at 37 °C. From a qualitative perspective, the number of colonies is inversely proportional to the duration of plasma treatment.

frequency of 500 Hz and a $V_{p\text{-}p}$ of ± 2.5 kV. It is worth mentioning that the conductive traces on the touchpad were at least 2.5 mm away from each other. Narrower gaps resulted in discharges and nonuniform ablation of the conductive layer of aluminum during activation. Movie S3 shows this demonstration in motion.

Kirigami-Like Plasma Generators. Kirigami uses the cutting of paper to create decorative or functional objects. As a proof-of-concept example, we created a kirigami-based device with an initial geometry of a 2D square as shown in Fig. 5*C*. When stretched, it opened into a 3D structure. The excitation frequency of this device was 500 Hz while the peak-to-peak voltage was ±2.5 kV. Kirigami-based devices might be useful for building conformable electronics that require stretching or bending about more than one axis.

Conclusions

In this article, we have introduced a concept for antimicrobial sanitization with flexible and disposable plasma generators made of paper. The design is simple, with back-to-back bonding of two sheets of metallized paper. The porosity of paper allows gas to permeate its bulk volume and fuel plasma, while forced convection cools the substrate. These mechanisms suggest fibrous, paper-like substrates may be appropriate in the design and fabrication of flexible devices to produce both volume and surface plasmas capable of killing microbes. With oscillating peak-to-peak potentials ranging from ±1 to ±10 kV, the paper-based plasma generators deactivated greater than 99% of *S. cerevisiae* and greater than 99.9% of *E. coli* cells with 30 s of treatment on neighboring substrates with an offset distance of 10 mm. We have also demonstrated how paper-based generators are conformable to curved surfaces, suitable for sanitization of aerosolized microbes onto a substrate, appropriate for kirigami-like stretchy structures, and compatible with user interfaces. In the future, paper-based plasma generators may be appropriate as antimicrobial protectors for skin-like sensors, self-sterilizing garments, devices for sterilizing laboratory or biomedical equipment, smart bandages for wound healing, or sacrificial components in manufacturing processes that apply patterned surface treatments.

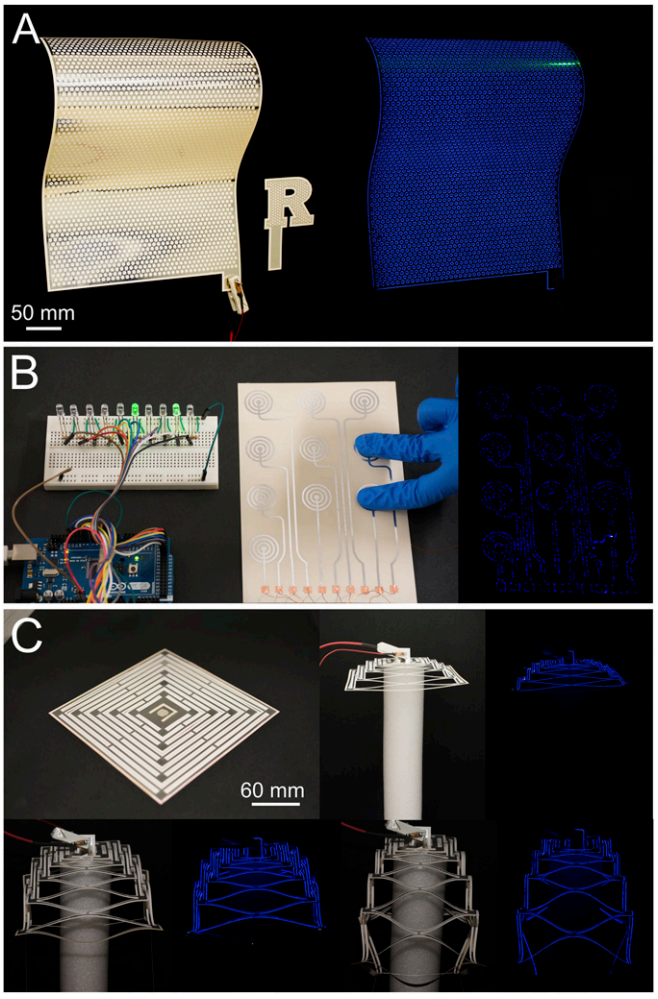

Fig. 5. Scalable and multifunctional plasma sanitizers made from metallized paper. (*A*) A 400-mm × 276-mm rectangular, paper-based plasma generator with a surface area ∼20 times larger than the R-shaped plasma generator shown in Fig. 1. The streak of green light in the upper right was from an external source. (*B*) A paper-based, capacitive touchpad served as an input device and plasma generator. (*C*) A kirigami-like plasma generator transformed from a planar to a 3D geometry.

Materials and Methods

Strains of Microbes. *Saccharomyces cerevisiae* strain AH109 (Clontech Laboratories) and *Escherichia coli strain* TOP10 (Invitrogen) served as samples of fungus and bacteria in our experiments. *S. cerevisiae* strain AH109 is a yeast strain usually used for two-hybrid screening in biological research. *E. coli* TOP10 is an ideal bacterial strain for high-efficiency cloning and plasmid propagation.

Preparation of Media and Microbes. We cultured *S. cerevisiae* strain AH109 and *E. coli* strain TOP10 with YEPD medium and LB medium, respectively. The YEPD broth contained 1% [mass/volume (m/vol)] yeast extract (Difco; Becton Dickinson), 2% (m/vol) peptone (Sigma-Aldrich), 2% (m/vol) dextrose (VWR International), and the rest was distilled water. The YEPD solid medium consisted of 0.3% (m/vol) yeast extract, 1% (m/vol) peptone, 1% (m/vol) dextrose, 2% (m/vol) agar (Difco; Becton Dickinson), with the rest being distilled water. We prepared LB medium with the dehydrated culture media of LB (powder form) (Difco; Becton Dickinson) and proper hydration with distilled water. The prepared LB medium contained 2.5% (m/vol) LB powder, and the rest was distilled water. The LB solid medium consisted of 2.5% (m/vol) LB powder, 1.5% (m/vol) agar, with the rest being distilled water. Autoclavation of all media lasted for 20 min at 121 °C. In the solid media of both YEPD and LB, it contained 25 mL of media in each Petri dish.

We cultured *S. cerevisiae* and *E. coli* in YEPD broth and LB broth, respectively, at 150 rpm in an orbital incubator shaker (model 3527; Lab-Line Instrumentations). The culturing lasted for 24 h at room temperature (25 °C). We collected the microbes by centrifuging (Clinical 100; VWR International) the cultures at 4,000 rpm ($\sim$1,520 $\times$ *g*) for 5 min. Both *S. cerevisiae* and *E. coli* cells were in suspension with sterilized distilled water. To determine the concentration of *S. cerevisiae* and *E. coli* in the suspension, we used a spectrophotometer (Genesys 10s UV-VIS; Thermo Scientific) to measure the value of OD_{600}, which indicated the optical density of samples measured at a wavelength of 600 nm. The measured OD_{600} of *S. cerevisiae* and *E. coli* were 1.037 and 0.867, indicating concentrations of $\sim 6.22 \times 10^7$ and 6.94×10^8 cells per mL, respectively. Finally, the concentrations were diluted to 2.07×10^3 and 2.50×10^4 cells per mL, respectively.

Image Acquisition. Unless otherwise specified, this work used a Nikon D7100 camera with an 18- to 105-mm lens to acquire images. For some still images of the plasma, we used extended exposure. The only digital modification of images was in contrast and brightness.

ACKNOWLEDGMENTS. We thank Wilson Rodriguez and Kris Mohan from Rutgers Environmental and Occupational Health Sciences Institute for providing equipment for ozone measurements. We also thank the anonymous reviewers for their helpful suggestions and comments. Joe Formosa from AR Metallizing, Ltd. (A Nissha Company), provided the metallized paper. Maxim Lazoutchekov helped with initial experimental measurements of the dielectric strength of the metallized paper. We acknowledge support from National Science Foundation Award 1610933 and from Rutgers University through the School of Engineering, the Department of Mechanical and Aerospace Engineering, the University Research Council, and an A. Walter Tyson Assistant Professorship Award. We acknowledge support from the John E. and Christina C. Craighead Foundation, US Department of Agriculture–National Institute of Food and Agriculture Multistate Project W3147, and the New Jersey Agricultural Experiment Station. S.R.'s work was partially supported by Air Force Office of Scientific Research Grant FA9550-15-1-0424.

1. Fauchais P (2004) Understanding plasma spraying. *J Phys Appl Phys* 37:R86–R108.
2. Li R, Ye L, Mai Y-W (1997) Application of plasma technologies in fibre-reinforced polymer composites: A review of recent developments. *Compos Part Appl Sci Manuf* 28:73–86.
3. Moisan M, et al. (2002) Plasma sterilization. Methods and mechanisms. *Pure Appl Chem* 74:349–358.
4. Halfmann H, Bibinov N, Wunderlich J, Awakowicz P (2007) A double inductively coupled plasma for sterilization of medical devices. *J Phys Appl Phys* 40:4145–4154.
5. Brewer GR (1962) Ion propulsion in space. *Nav Eng J* 74:373–377.
6. Martinez-Sanchez M, Pollard JE (1998) Spacecraft electric propulsion-an overview. *J Propuls Power* 14:688–699.
7. He C, Corke TC, Patel MP (2009) Plasma flaps and slats: An application of weakly ionized plasma actuators. *J Aircr* 46:864–873.
8. Moreau E (2007) Airflow control by non-thermal plasma actuators. *J Phys Appl Phys* 40:605–636.
9. Zhao P, Portugal S, Roy S (2015) Efficient needle plasma actuators for flow control and surface cooling. *Appl Phys Lett* 107:33501.
10. Lloyd G, et al. (2010) Gas plasma: Medical uses and developments in wound care. *Plasma Process Polym* 7:194–211.
11. Gallagher MJ, et al. (2007) Rapid inactivation of airborne bacteria using atmospheric pressure dielectric barrier grating discharge. *IEEE Trans Plasma Sci* 35:1501–1510.
12. Mastanaiah N, Banerjee P, Johnson JA, Roy S (2013) Examining the role of ozone in surface plasma sterilization using dielectric barrier discharge (DBD) plasma. *Plasma Process Polym* 10:1120–1133.
13. Laroussi M (2009) Low-temperature plasmas for medicine? *IEEE Trans Plasma Sci* 37: 714–725.
14. Kogelschatz U (2003) Dielectric-barrier discharges: Their history, discharge physics, and industrial applications. *Plasma Chem Plasma Process* 23:1–46.
15. Huang C (2006) An experimental investigation of low temperature plasma sterilization, treatment, and polymerization processes. PhD dissertation (University of Missouri, Columbia, MO).
16. Lerouge S, Wertheimer M, Yahia L (2001) Plasma sterilization: A review of parameters, mechanisms, and limitations. *Plasmas Polym* 6:175–188.
17. McDonnell GE (2007) *Antisepsis, Disinfection, and Sterilization* (American Society of Microbiology, Washington, DC).
18. Henn GG, Birkinshaw C, Buggy M, Jones E (1996) A comparison of the effects of γ-irradiation and ethylene oxide sterilization on the properties of compression moulded poly-D,L-lactide. *J Mater Sci Mater Med* 7:591–595.
19. Morrissey RF, Herring CM (2002) Radiation sterilization: Past, present and future. *Rad iat Phys Chem* 63:217–221.
20. Zimek Z, Kaluska I (1998) Economical aspects of radiation sterilization with electron beam. *Radiat Technol Conserv Environ* 1998:457.
21. Silindir M, Özer AY (2009) Sterilization methods and the comparison of E-beam sterilization with gamma radiation sterilization. *Fabad J Pharm Sci* 34:43–53.
22. Mastanaiah N, Johnson JA, Roy S (2013) Effect of dielectric and liquid on plasma sterilization using dielectric barrier discharge plasma. *PLoS One* 8:e70840.
23. Morfill GE, Shimizu T, Steffes B, Schmidt H-U (2009) Nosocomial infections—a new approach towards preventive medicine using plasmas. *New J Phys* 11:115019.
24. Zimmermann JL, et al. (2011) Effects of cold atmospheric plasmas on adenoviruses in solution. *J Phys Appl Phys* 44:505201.
25. Kim DY, Park C, Leem J, Kim S (2014) Raw food sterilization of flexible dielectric barrier discharge device using biocompatible tubing. *IEEE T Plasma Sci* 42:2758–2759.
26. Soares S, Camino G, Levchik S (1995) Comparative study of the thermal decomposition of pure cellulose and pulp paper. *Polym Degrad Stabil* 49:275–283.
27. Martinez AW, Phillips ST, Whitesides GM (2008) Three-dimensional microfluidic devices fabricated in layered paper and tape. *Proc Natl Acad Sci USA* 105:19606–19611.
28. Martinez AW, Phillips ST, Butte MJ, Whitesides GM (2007) Patterned paper as a platform for inexpensive, low-volume, portable bioassays. *Angew Chem Int Ed Engl* 46:1318–1320.
29. Pollock NR, et al. (2012) A paper-based multiplexed transaminase test for low-cost, point-of-care liver function testing. *Sci Transl Med* 4:152ra129.
30. Hu L, et al. (2009) Highly conductive paper for energy-storage devices. *Proc Natl Acad Sci USA* 106:21490–21494.
31. Kim DY, Steckl AJ (2010) Electrowetting on paper for electronic paper display. *ACS Appl Mater Interfaces* 2:3318–3323.
32. Mu J, et al. (2015) Origami-inspired active graphene-based paper for programmable instant self-folding walking devices. *Sci Adv* 1:e1500533.
33. Nie Z, et al. (2010) Electrochemical sensing in paper-based microfluidic devices. *Lab Chip* 10:477–483.
34. Dungchai W, Chailapakul O, Henry CS (2009) Electrochemical detection for paper-based microfluidics. *Anal Chem* 81:5821–5826.
35. Mazzeo AD, et al. (2012) Paper-based, capacitive touch pads. *Adv Mater* 24: 2850–2856.
36. Maxwell EJ, Mazzeo AD, Whitesides GM (2013) Paper-based electroanalytical devices for accessible diagnostic testing. *MRS Bull* 38:309–314.
37. Siegel AC, et al. (2010) Foldable printed circuit boards on paper substrates. *Adv Funct Mater* 20:28–35.
38. Tian H, et al. (2011) Graphene-on-paper sound source devices. *ACS Nano* 5:4878–4885.
39. Hales TC (1999) The honeycomb conjecture. *Discrete Comput Geom* 25:1–22.
40. Laroussi M (1996) Sterilization of contaminated matter with an atmospheric pressure plasma. *IEEE Trans Plasma Sci* 24:1188–1191.
41. Duguid JP (1946) The size and the duration of air-carriage of respiratory droplets and droplet-nuclei. *J Hyg (Lond)* 44:471–479.
42. Magill SS, et al.; Emerging Infections Program Healthcare-Associated Infections and Antimicrobial Use Prevalence Survey Team (2014) Multistate point-prevalence survey of health care-associated infections. *N Engl J Med* 370:1198–1208.
43. Fischer WA, 2nd, Weber DJ, Wohl DA (2015) Personal protective equipment: Protecting health care providers in an Ebola outbreak. *Clin Ther* 37:2402–2410.
44. Edmond MB, Diekema DJ, Perencevich EN (2014) Ebola virus disease and the need for new personal protective equipment. *JAMA* 312:2495–2496.
45. Verbeek JH, Mihalache RC (2016) More PPE protects better against Ebola. *Am J Infect Control* 44:731.
46. Laroussi M, Alexeff I, Richardson JP, Dyer FF (2002) The resistive barrier discharge. *IEEE Trans Plasma Sci* 30:158–159.
47. Williamson JM, Trump DD, Bletzinger P, Ganguly BN (2006) Comparison of high-voltage ac and pulsed operation of a surface dielectric barrier discharge. *J Phys Appl Phys* 39:4400–4406.
48. Kogelschatz U, Eliasson B, Hirth M (1988) Ozone generation from oxygen and air: Discharge physics and reaction mechanisms. *Ozone Sci Eng* 10:367–377.

Supporting Information

Xie et al. 10.1073/pnas.1621203114

Measurement of Absolute Irradiance of Emitted UV Light

To characterize emitted electromagnetic radiation from the plasma generator and the corresponding absolute irradiance, we used a spectroradiometer (USB2000+; Ocean Optics) calibrated for wavelengths ranging from 200 to 850 nm to perform the measurements. It had a cosine corrector-attached fiber mounted 2 mm away and perpendicular to the surface of the plasma generator. Such a distance enabled the measurement over a single hexagonal cell on the plasma generator. By multiplying the measurements on a single cell by the total number of hexagonal cells on a plasma generator, we obtained the total irradiance.

As shown in Fig. S1, the highest peaks occurred for wavelengths between 315 and 400 nm in the UV A (UVA) regime. Multiple peaks occurred between 400 and 500 nm, which correspond to the visible blue and violet colors captured in photographs. There were also detectable levels of UV B (UVB) and UV C (UVC) from the plasma generator. Previous studies have shown that UVC is one of the critical factors in disinfection technologies (23, 24).

Measurement of Ozone Level

As introduced in previous work (47), when dielectric barrier discharge is in progress, the reaction of free oxygen atoms with oxygen generates a significant amount of ozone based on the following reaction:

$$O + O_2 + M \rightarrow O_3 + M, \qquad \textbf{[S1]}$$

where M is an involved collision partner, such as O_2, O_3, and N_2 (48). The highly reactive ozone can also react with oxygen atoms created from the electron impact dissociation of O_2:

$$O_3 + O + M \rightarrow 2O_2 + M. \qquad \textbf{[S2]}$$

The experimental setup for characterizing ozone level in atmospheric environment consists of three major components: an enclosed glass chamber (35 cm × 35 cm × 63 cm), a fast response UV-based ozone monitor (model 205; 2B Technologies), and a LabVIEW-based (LabVIEW 2014; National Instruments) high-speed data acquisition system (NI 9215; National Instruments). To measure the ozone concentration, we placed a circular paper-based plasma sterilizer at one lower corner of the chamber. The intake tubing of the ozone monitor sat in the center of the chamber. Both of them sat on the floor. The ozone monitor recorded two samples per second with a resolution of 0.1 ppb. Fig. S3 depicts the experimental setup.

We measured the profiles of ozone level for 40 min with plasma activated for 5, 10, 20, 30, 60, and 120 s. The AC input to all of the devices had a frequency of 2 kHz and a peak-to-peak voltage of 6.3 kHz. The ozone concentration, with plasma activation for different lengths of time, arrived at peak values within the first 200 s. It then decayed to a much lower level of ∼50 ppb after 2,000 s (about 33 min). Table S1 shows the peak values of ozone level for each measurement.

Although ozone level is dependent on the size of the space over which we conducted the measurements, the experimental results demonstrated that the paper-based plasma sterilizer was able to generate a significant amount of ozone within a short time as shown in Table S1 and Fig. S2*A*. In addition to these measurements of ozone, we also conducted specific measurements to detect the ozone concentration in a circular Petri dish, which has a diameter of 100 mm and a thickness of 15 mm. However, within such a limited space, the ozone quickly—within seconds—accumulated to values out of the measurable range (200 ppm) of the ozone monitor.

Measurement of Surface Temperature

Temperature is one of the controlled parameters in conventional approaches to disinfection, such as pasteurization. In this work, we targeted low surface temperatures with plasma-based sanitization. The increase of surface temperature results mainly from Joule heating in the layer of aluminum. To characterize the changing surface temperature, we used an Arduino-based temperature logging system to track the change of temperature. A precalibrated noncontact IR thermometer (MLX90614; Melexis Microelectronic Systems) monitored the change of temperature at a distance of 2 cm pointing to the center of the circular plasma sterilizer, which is identical to the ones we used in noncontact experiments, at an ambient temperature of 25 °C.

Fig. S2*B* shows the surface temperature as a function of time. With a fixed frequency of 2 kHz and varied voltages $V_{P\text{-}P}$ ranging from ±1.5 to ±3 kV, the surface temperature did not exceed 60 °C after a 60-s activation of the plasma generator.

Customizable Paper-Based Generators

One of the advantages of paper-based plasma generators is its capability of sanitizing adjacent objects in addition to itself. Moreover, the use of paper as the substrate for plasma generators enables the customizability of devices. To demonstrate these features, we prepared another paper-based plasma generator with the geometry of the spirit mark of Rutgers, a capitalized letter "R." As Fig. S4 shows, we adopted the pattern of repeated hexagons to provide coverage with plasma over the entirety of the surface.

To perform these experiments, we first aerosolized a suspension of *E. coli* onto one side of a sterilized, circular polyethylene terephthalate (PET) film (Mylar 201; DuPont Teijin Films) with a diameter of 135 mm. Then, we placed it on the top of a sterilized glass plate sitting in a recirculating hood. When the surface of the PET film was dry, we placed the R-shaped plasma generator on the surface of the film with the hexagonal pattern facing the film. Next, we gently placed a glass cover on it. The purpose of using the glass cover was to ensure the flatness of the R-shaped plasma generator. Fig. S4*A* shows the setup at this step.

With an AC source ($V_{p\text{-}p}$ = ±3 kV, f = 1.7 kHz), we activated the plasma for 10, 20, 30, and 60 s. After removing the plasma generator, we transferred *E. coli* cells by attaching the top surface of the PET film onto the surface of LB medium in a Petri dish. The medium went through a 24-h incubation at 37 °C. Fig. S4*B* shows the distribution of *E. coli* on the LB medium after a treatment of 10 s. The central area previously covered and sanitized by the R-shaped, paper-based plasma generator exhibited only several colonies of *E. coli*, whereas the uncovered area yielded numerous colonies. Moreover, even though the plasma generator had a specific geometry that could presumably result in a sanitized, R-shaped region free of *E. coli* cells, the result did not present such a region. This lack of geometric definition was mainly because of the absence of precise control of the plasma, which is convective and diffusive in fluidic nature. Movie S1 demonstrates the experiments described in this section. Movie S4 demonstrates plasma-based convective flows.

Disinfection of Tools and Equipment

We performed rigorous disinfection on all of the tools, including tweezers, inoculation loops, scissors, etc., by submerging them in ethanol with a concentration of 99%. Then, they went through a

flame for further disinfection before use. The circular paper-based plasma generators sat in a UV disinfection cabinet for 5 h before use. We performed all of the experiments in a recirculating fume hood.

Characterization of Dielectric Strength

As the application of high electric fields was capable of leading to dielectric breakdown of the plasma generators, we characterized the dielectric strength of metallized paper. As shown in Fig. S5 *A*–*C*, there were three types of samples (i.e., single layer, double layers with a "top-to-bottom" configuration, and double layers with a "bottom-to-bottom" configuration). For simplicity, "top" refers to the upper, aluminum conductive layer of metallized paper, and "bottom" refers to the lower, cellulose fiber layer of the metallized paper. It is worth mentioning that, in the double-layer configurations, a minimum margin with a width of 3 mm from the edges of one layer to the other is necessary to avoid direct discharge between the two aluminum layers. This possible discharge is mainly because the dielectric strength of air (3.0 MV/m) is lower than that of the composite of polymers and cellulose fibers in the metallized paper.

To characterize the dielectric strength, we first used a "short-time" method by placing a sample between two electrodes and by gradually increasing the voltage across both sides of the metallized paper until a breakdown occurred. Then, we used a "slow rate-of-rise" method to acquire more accurate breakdown voltages by gradually increasing the voltage from 50% of the breakdown voltage determined in the previous short-time method until breakdown. The dielectric strength of a single layer had mean values between 10 and 50 MV/m based on five measurements at frequencies ranging from 0.01 to 30 kHz. For a two-layer structure with a top-to-bottom configuration, the mean value of dielectric strength was between 40 and 56 MV/m at frequencies ranging from 0.01 to 10 kHz. For a two-layer structure with a bottom-to-bottom configuration, the mean value of dielectric strength was between 55 and 82 MV/m at frequencies ranging from 0.1 to 10 kHz. When the frequency approached 0.01 kHz, the breakdown voltage for the bottom-to-bottom configuration was higher than the maximum provided voltage (±10 kV) from the power supply system. Fig. S5*D* shows the measured results of the samples.

Self-Sanitization with Volume Plasma

Volume plasma facilitates the sanitization of contaminants residing in the fibrous interior of paper-based devices. To investigate the role of volume plasma in self-sanitization, we conducted an additional set of experiments by intentionally contaminating the nonpatterned, paper-based plasma generators (Fig. 1 *F* and *G*) with dry spores of an airborne *Penicillium* sp., and then activating plasma for 2 min with a $V_{p\text{-}p}$ of ±2.5 kV at 2 kHz. Immediately after the treatment, we split the samples along the centerline and transferred the spores at the edge to potato dextrose agar (Neogen Corporation). Fig. S6 *A*–*F* illustrates the procedure of the experiments. The microscopic image in Fig. S6*A* shows the asexual reproductive structures [i.e., conidiophore, asexual spores (conidia)]. We stained the sample with 1% aniline blue solution to make it prominent.

Fig. S6 *G* and *H* shows the comparison between an experimental group and a control group after 48 h of incubation at 30 °C. The two edges in the experimental group were free of colonies/spores of the *Penicillium* sp., whereas the edges in the control group had colonies/spores growing.

To identify the specific species of the *Penicillium*, we extracted DNA from the isolated fungus obtained from the control group. Then, we conducted PCR with two primers, LR3R (5′-GTCTTGAAACACGGACC-3′) and LR5 (5′-TCCTGAGGGAAACTTCG-3′), to amplify a 310-bp conserved region of 5.8S ribosomal RNA. The purified PCR product went to GENWIZE for sequencing, and the results were analyzed with the Basic Local Alignment Search Tool (BLAST) from the National Center for Biotechnology Information. The result showed the 638- to 948-bp 5.8S rRNA region of the isolated fungus matched the same region of many *Penicillium citrinum* isolates. Both molecular and morphological results indicate that the fungus is a *Penicillium citrinum* species.

Flexibility

To test the flexibility of paper-based generators, we used straight tubes with varied radii ranging from $R = 9.5$ mm to $R = 46$ mm and attached generators to the surfaces of these tubes (Fig. S7). With a peak–peak voltage $V_{p\text{-}p}$ of ±3.15 kV at 2 kHz (the same AC input we applied to generators produced for the biological experiments), the paper-based sanitizers still functioned and produced plasma. However, when attached to a tube with $R =$ 3.2 mm, the device was not able to generate plasma because of cracking in the aluminum layer of the paper.

Durability of Paper-Based Sanitizers

We attached a circular paper-based sanitizer to a segment of a cylindrical, polyethylene piece of foam with a diameter of 75 mm. Next, we fixed the sample inside a closed desiccator (Nalgene; Thermo Scientific) with an internal volume of 10.2 L. Then, we inserted the gas inlet of an ozone monitor to the container (Fig. S8*B*). To test the durability of the paper-based sanitizer, we activated the plasma for 30 s, and then stopped and waited until the level of ozone dropped to lower than 200 ppb over ∼20 min. We performed eight repetitive cycles with a $V_{p\text{-}p}$ of ±3.15 kV at 2 kHz. During each trial, the ozone monitor logged data continuously with an averaging time of 2 s over the recorded raw data. Fig. S8*A* shows that there may have been a break-in period for the device, as the first trial produced less ozone than that measured in subsequent trials.

Sanitization at Varied Distances

Fig. 2 shows the effective deactivation of both *S. cerevisiae* and *E. coli* with paper-based sanitizers 10 mm away from the surface of the agar. To investigate the effect of varied distances on the effectiveness of sanitization, we performed two additional sets of noncontact experiments with circular, paper-based sanitizers 10 and 20 mm away from the surface of agar (Fig. S9*A*). The microbes used in the additional experiments were *S. cerevisiae* with a concentration of $\sim 1 \times 10^4$ cells per mL. Both sets of experiments shared the same times of treatment and AC input ($V_{p\text{-}p} = \pm 3.15$ kV, $f = 2$ kHz) to the paper-based sanitizers. For each of the six test groups, there were seven repetitive samples. Immediately after timed treatment, we incubated each sample at 30 °C for 48 h.

Fig. S9*B* shows the experimental results. When the distance was 20 mm, the effectiveness of sanitization resembled that when the distance was 10 mm—in fact, there were slightly higher degrees of deactivation of *S. cerevisiae* cells within the same amount of time in each group, except the ones with 120-s treatment. One plausible explanation is that ozone is the dominating factor in sanitization with these paper-based devices at these distances. Within the larger Petri dishes, there were larger initial quantities of air than in the smaller Petri dishes. With more fuel available in larger Petri dishes, it is possible that the plasma generators were able to convert the readily available fuel quickly into ozone to create similar concentrations of ozone in the Petri dishes within 10 s of activated treatment. Thus, the experimental results suggest that distance may not affect the effectiveness of sanitization, as long as the enclosed space fills quickly with a high concentration of ozone produced by the plasma generators.

Boiling Versus Plasma Treatment

As an alternative technology for sanitization/sterilization, plasma might avoid potential damage to surfaces/structures of objects under treatment that might occur with conventional technologies.

To demonstrate this point, we conducted two experiments—one used boiling, and the other used plasma—to treat two samples made of a heat-shrinking polyolefin. At elevated temperatures as low as 70 °C, a heat-shrinking polyolefin can experience significant changes in its size. Therefore, deactivating microbes on surfaces of polyolefins might not be ideal with heat or boiling water. As Fig. S10*A* shows, the sample shrank significantly in boiling water at 100 °C for only 2 s. In contrast, a sample in direct contact with a paper-based plasma generator did not exhibit observable shrinkage when treated for 60 s as shown in Fig. S10*B*.

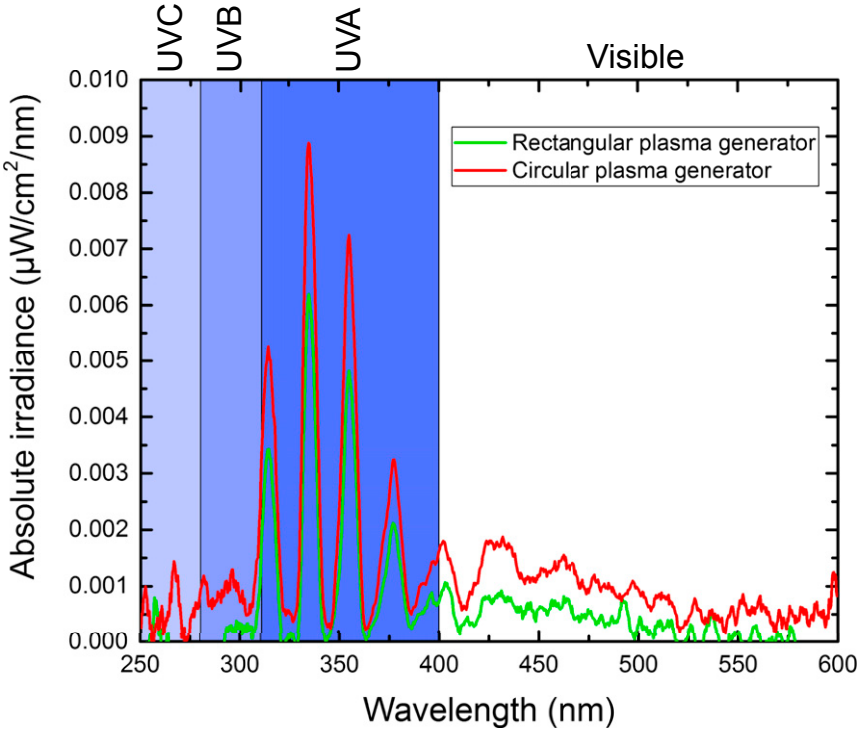

Fig. S1. Spectrophotography of the emitted electromagnetic waves from a rectangular and a circular flexible plasma generator.

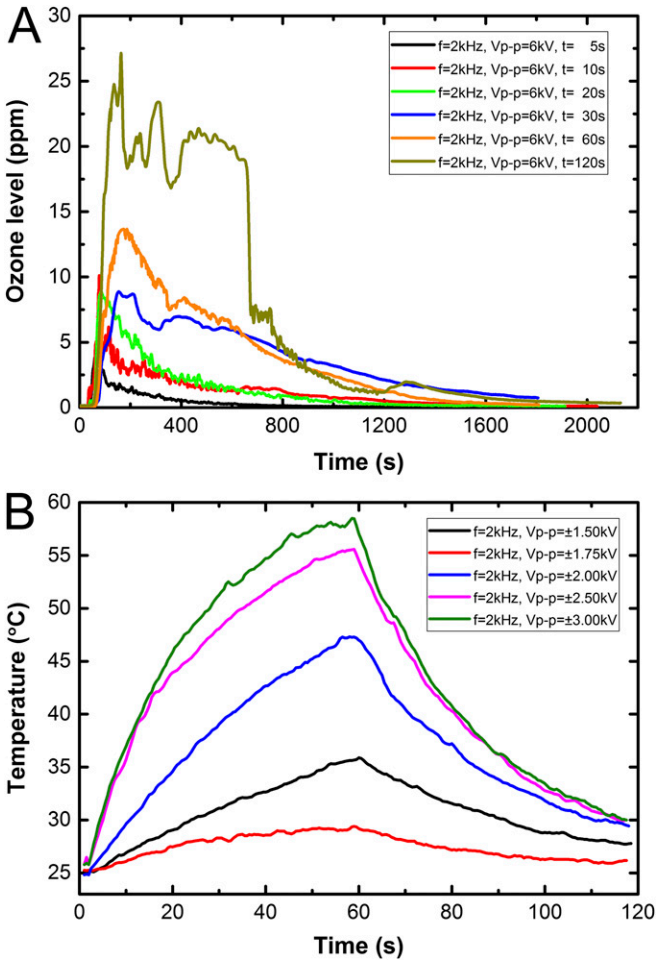

Fig. S2. Measurements of ozone generated from paper-based plasma generators. (*A*) Plotted ozone level as a function of time with varied activation times indicated in the legend. (*B*) Plotted temperature on the paper-based plasma generator as a function of time with varied peak-to-peak voltage indicated in the legend for 60-s activation of plasma generators.

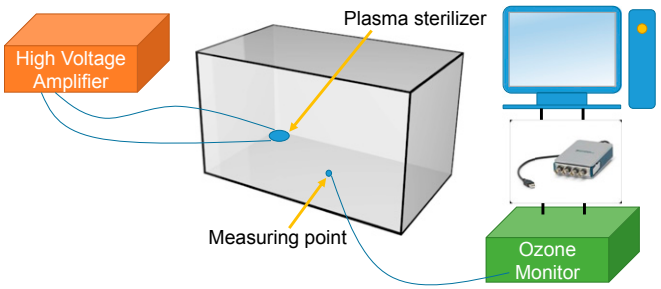

Fig. S3. Experimental setup for the measurement of ozone level.

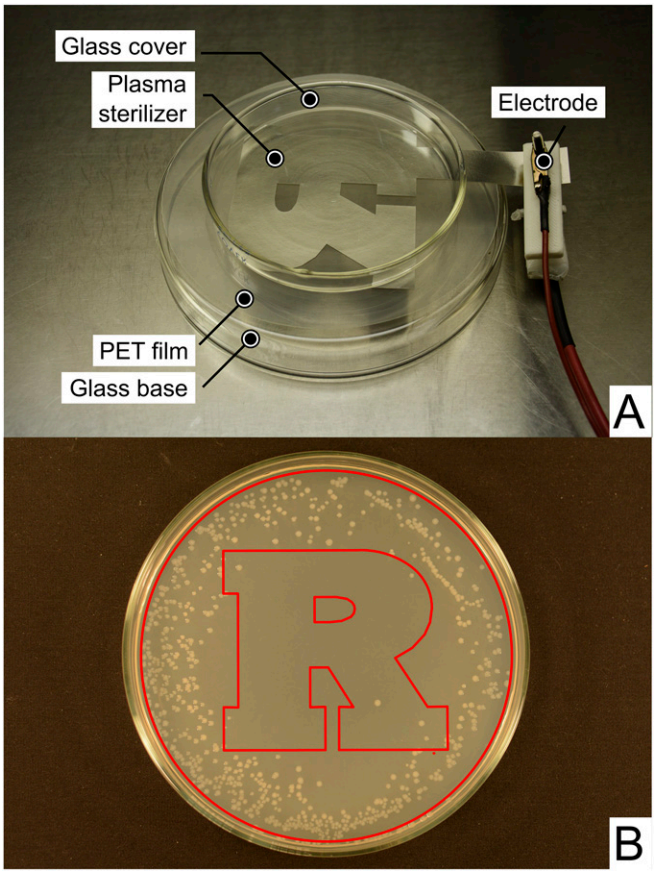

Fig. S4. The effectiveness of a customized, paper-based plasma generator. (*A*) The paper-based device in direct contact with a circular PET film sanitized *E. coli*. (*B*) After an incubation for 24 h at 37 °C, the area sanitized by the paper-based generator with a design of Rutgers spirit logo "R" presented very few colonies, whereas the uncovered area yielded a large number of colonies of *E. coli*. A red overlay serves to visualize the boundary of the PET film and the R-shaped, sanitized area.

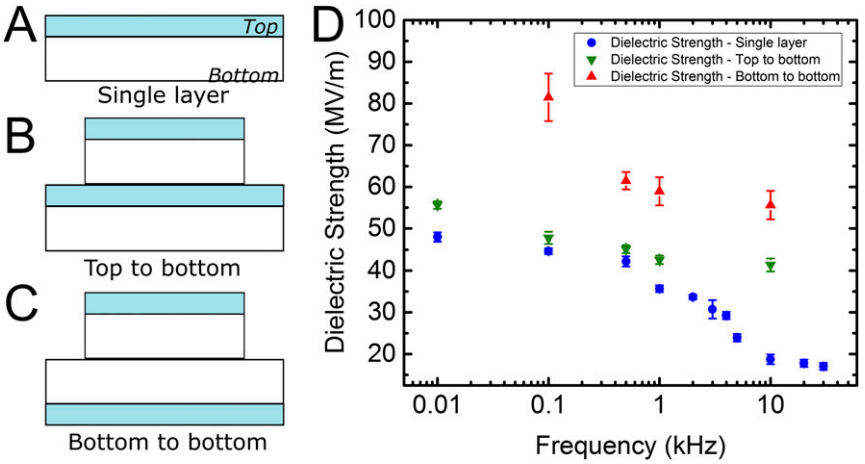

Fig. S5. Configuration of samples and measured results of dielectric strength. (*A–C*) The three types of configurations used in the characterization. (*D*) The dielectric strength as a function of frequency.

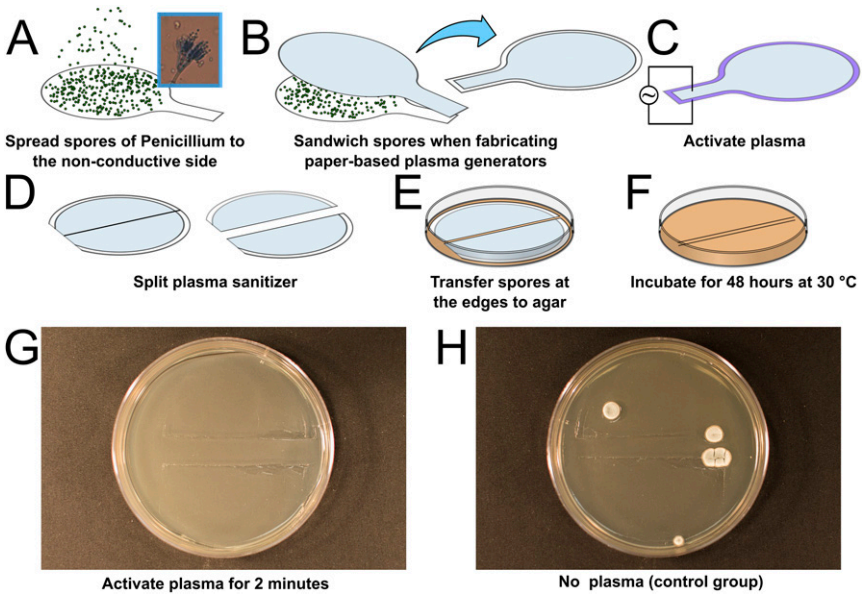

Fig. S6. An experiment showing the self-sanitizing effect of volume plasma. (*A*–*F*) The steps of preparing a contaminated paper-based plasma generator with spores of *Penicillium* and sanitizing the device with plasma. *G* and *H* show the experimental results. There were not visible colonies of *Penicillium* growing in the agar after 2 min of plasma treatment.

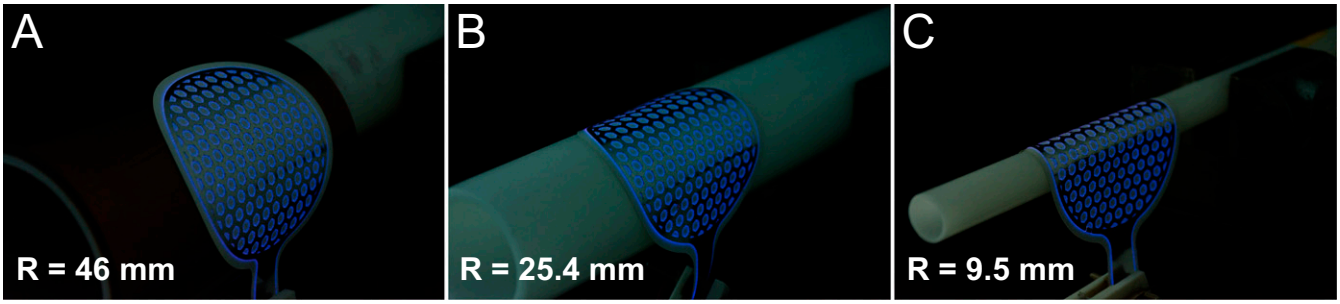

Fig. S7. Paper-based plasma generators attached to tubes with varied radii of (*A*) 46 mm, (*B*) 25.4 mm, and (*C*) 9.5 mm are still capable of producing plasma.

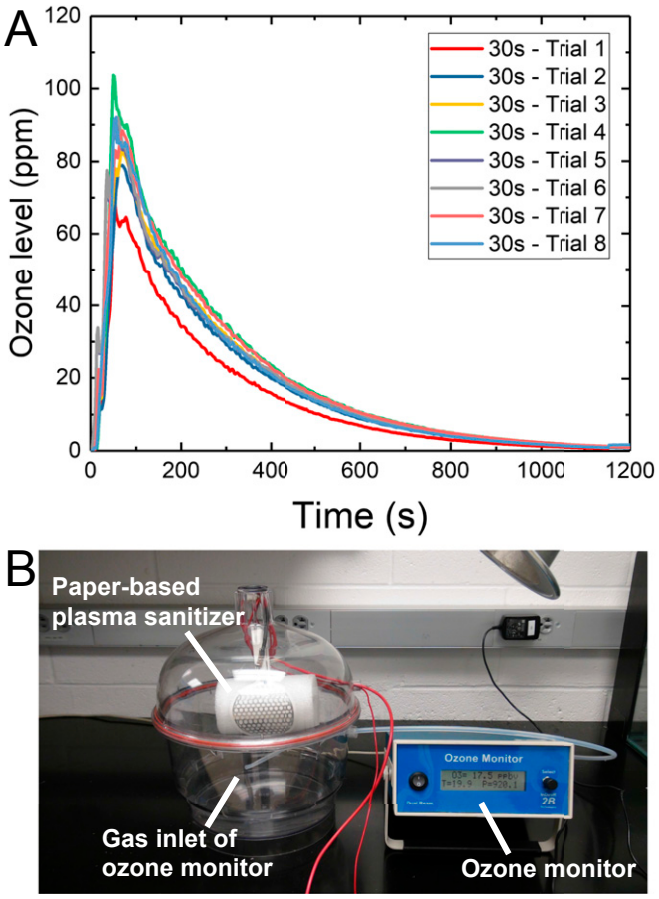

Fig. S8. (*A*) Plotted ozone level from eight measurements of a circular, paper-based sanitizer as a function of time. (*B*) The experimental setup shows the paper-based sanitizer attached to a segment of cylindrical foam made from polyethylene. The activation time was 30 s.

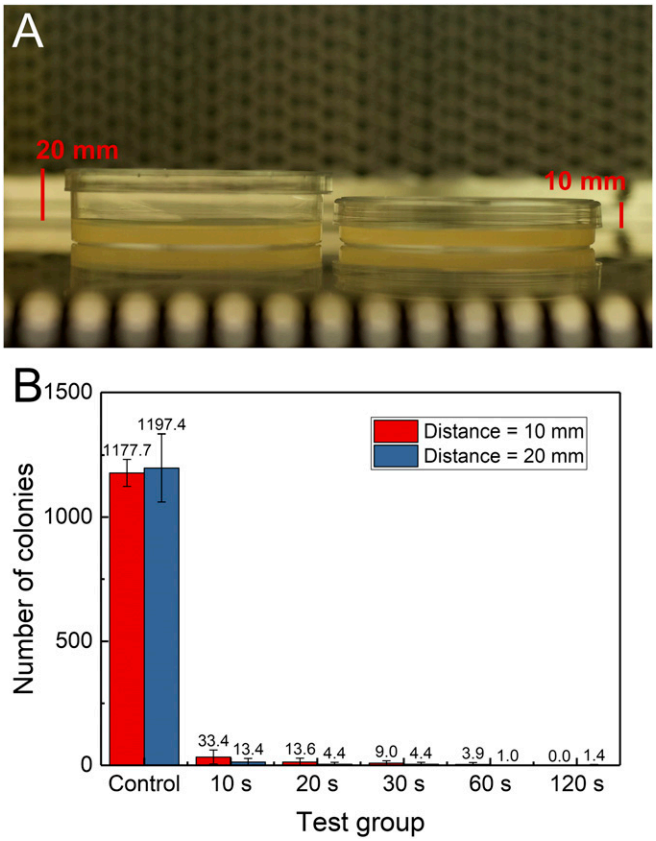

Fig. S9. (*A*) Two types of Petri dish used in noncontact experiments. The varied distances between the surfaces of plasma sanitizers and the agar were 10 and 20 mm, respectively. (*B*) Plotted number of colonies versus sanitization time from two groups of noncontact experiments on *S. cerevisiae* cells. The error bars represent ±1 SD calculated for seven repetitive experiments for each test group.

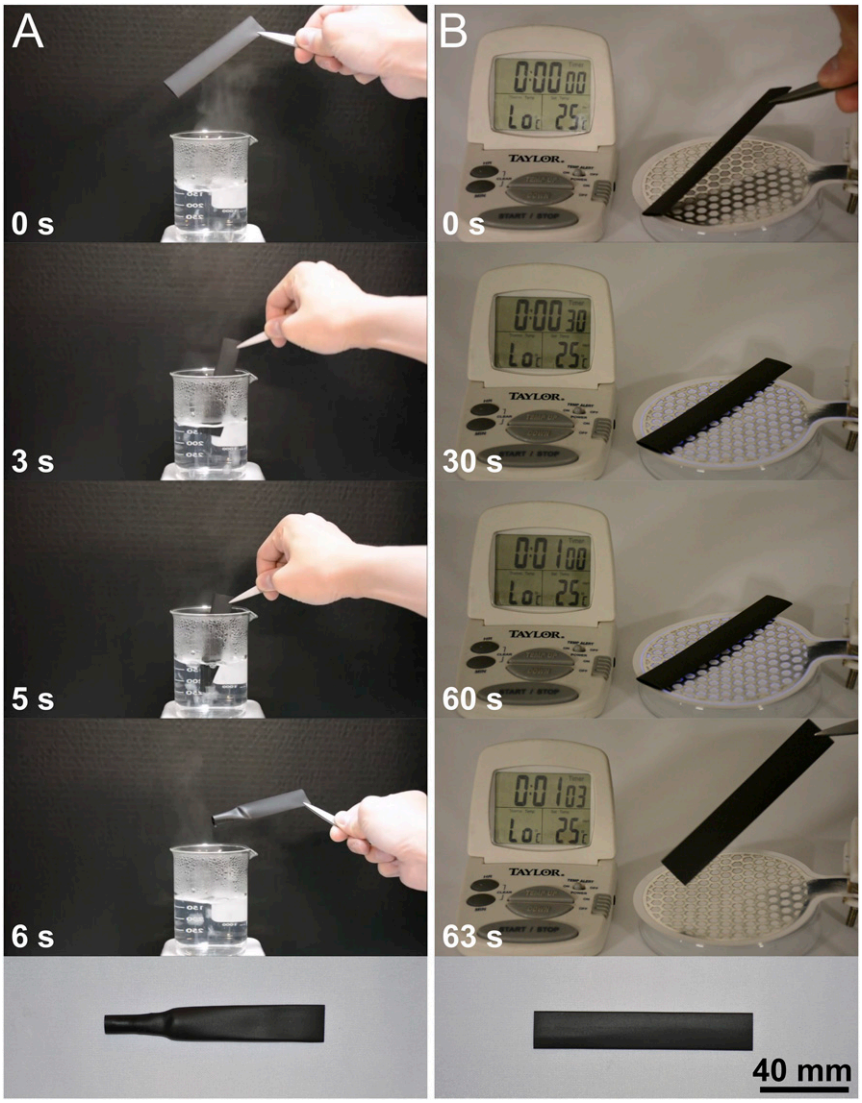

Fig. S10. A comparative study shows significant modification of material properties by using (*A*) boiling water and minimal modification with a (*B*) plasma sanitizer.

Table S1. Measured peak levels of ozone in an enclosed glass chamber (35 cm × 35 cm × 63 cm) with varied times of activated plasma

Time of activation, s	Peak ozone level, ppm
5	5.6
10	7.2
20	9.8
30	9.0
60	13.5
120	27.3

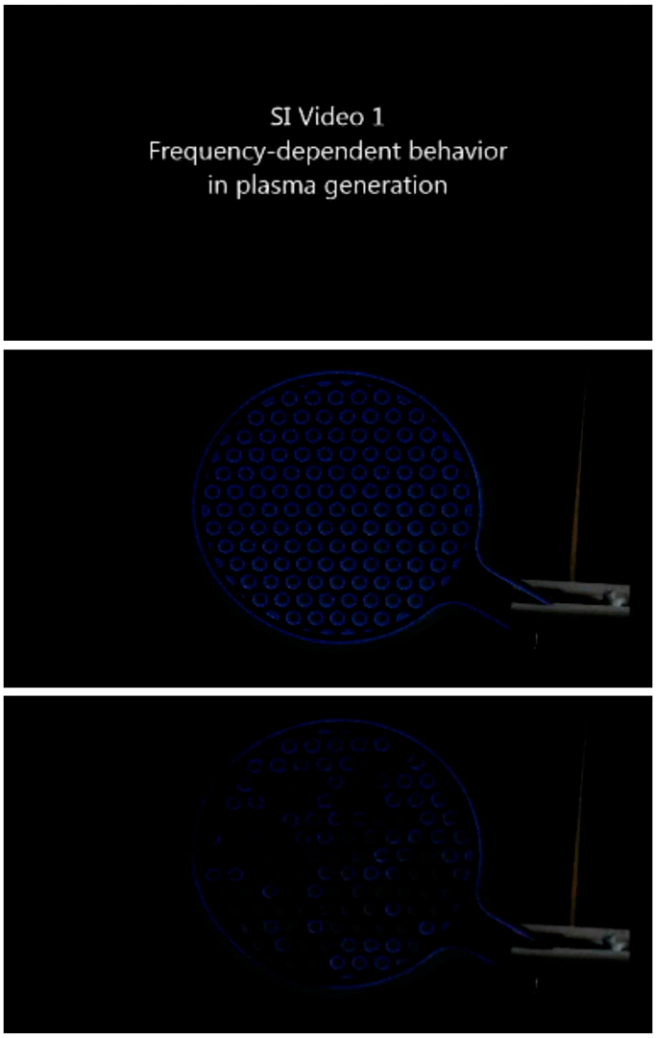

Movie S1. Frequency-dependent behavior in plasma generation. This movie demonstrates the plasma generation as a function of applied frequency at a constant potential $V_{p\text{-}p} = \pm 3$ V. It shows the varying coverage of plasma with the change of frequency ranging from 2 to 3.3 kHz. The second part of the video shows the same frequency dependency in normal lighting.

Movie S1

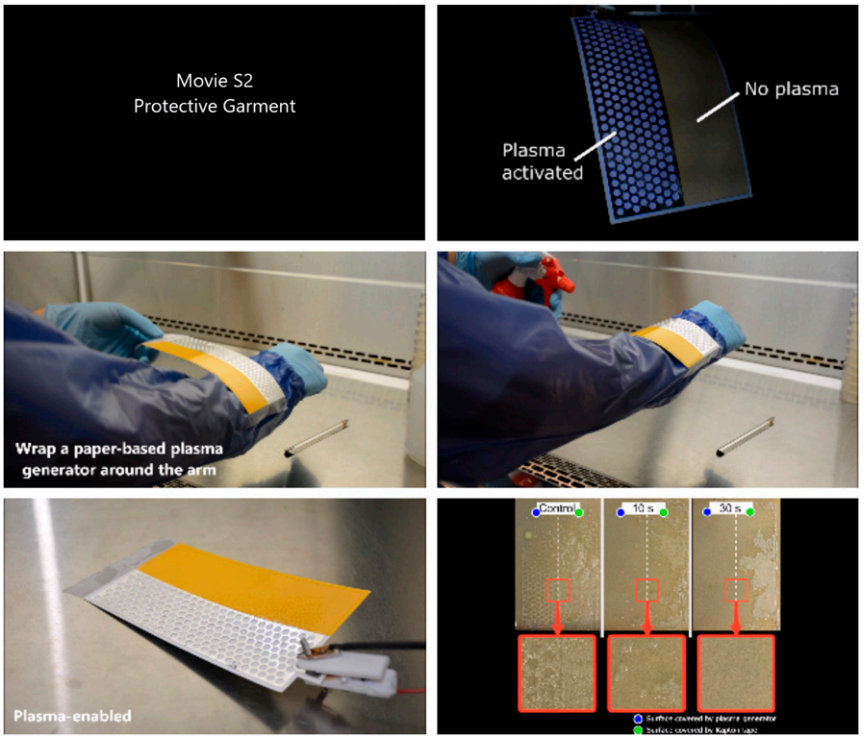

Movie S2. Protective garment. The use of paper-based plasma generator as a protective garment.

Movie S2

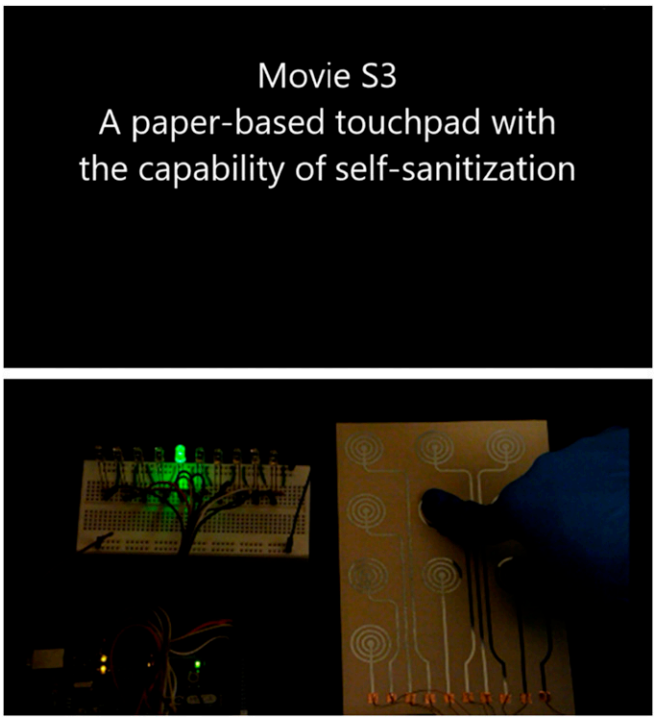

Movie S3. A paper-based touchpad with the dual functionality of generating plasma for potential self-sanitization.

Movie S3

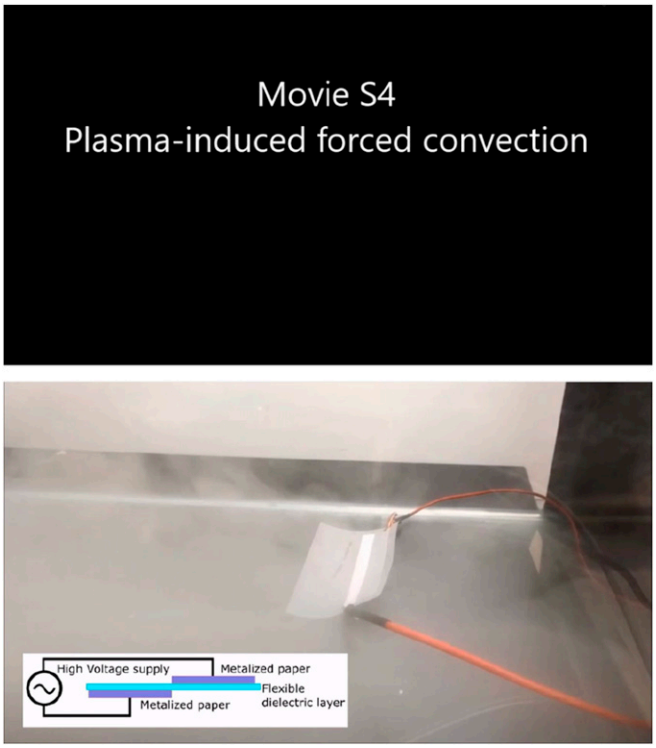

Movie S4. Plasma-induced forced convection. This movie is a qualitative demonstration of plasma-induced forced convection from a paper-based plasma generator. The effect of the induced flow is apparent on the surrounding fog. The diagram in the lower-left corner shows the cross-sectional view of the setup. A Sony HDR-CX760V camcorder acquired this movie.

Movie S4

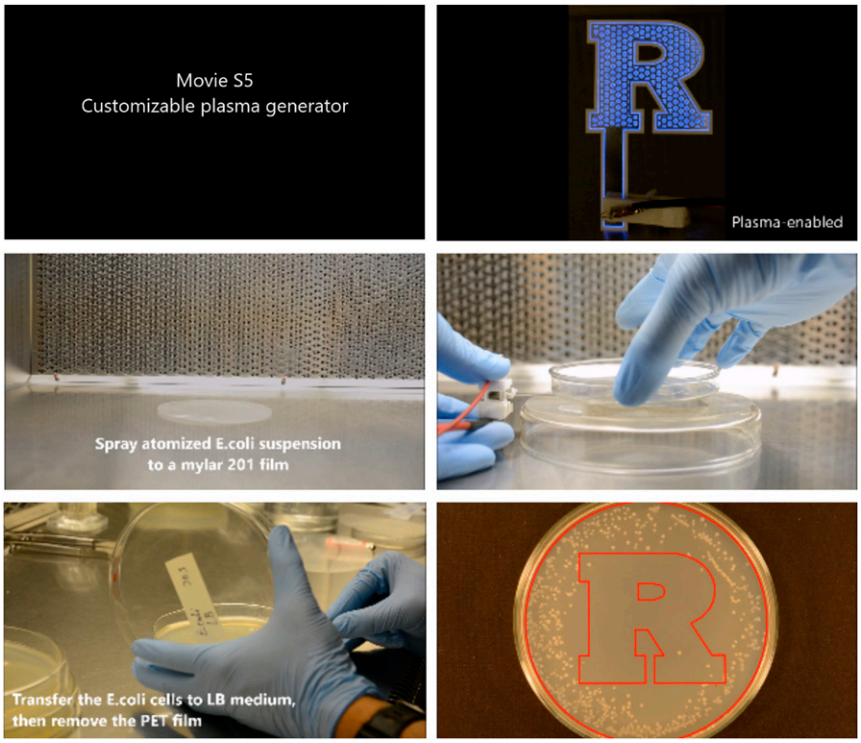

Movie S5. Customizable plasma generator. Direct-contact sanitization of a surface by using a paper-based plasma generator with a Rutgers logo-like design.

Movie S5